



2301-9069 (e)
1829-8370 (p)

Kapal: Jurnal Ilmu Pengetahuan dan Teknologi Kelautan (Kapal: Journal of Marine Science and Technology)

journal homepage: <http://ejournal.undip.ac.id/index.php/kapal>

Combining Optimum Propeller Design on Roro Ship Re-engine

I Made Ariana¹⁾, Adhi Iswantoro^{1*)}, Salsabilla Aulia Fitri¹⁾

¹⁾Department of Marine Engineering, Faculty of Marine Technology, Institut Teknologi Sepuluh Nopember, Surabaya 60111, Indonesia

^{*)}Corresponding Author: adhi.iswantoro@gmail.com



Article Info

Abstract

Keywords:

The algorithm;
CFD;
EPM;
optimum propeller;

Article history:

Received: 12/03/2023
Last revised: 18/05/2023
Accepted: 20/05/2023
Available online: 20/05/2023
Published: 20/05/2023

DOI:

<https://doi.org/10.14710/kapal.v20i2.52979>

Passenger ships serve several areas in Indonesia, one of which is KMP (*Kapal Motor Penumpang*) Dharma Rucitra 3. In 2020 this ship had an accident and almost sank, then causing the main engine to submerge. With this problem, it is necessary to repower the engine provided by the company by replacing the old engine with a new engine. The new engine, namely Yanmar 6N21A SV, with a power of 1200 HP at 850 RPM. Initially, the ship's speed was 12 knots with the data of Makita GNLH 630M engine with a power of 1300 HP at 375 RPM with a B4-50 propeller. To achieve the desired speed, it is necessary to have an optimal propeller to improve engine performance. In this research, an algorithm has been specially developed to find the optimum propeller design of B-series propellers for KMP Dharma Rucitra 3 by defining the overall parameters of a propeller-like diameter, pitch-ratio, blade area ratio and the number of blades. The optimum propeller design is performed as a multiobjective function to constraints imposed by propeller parameters. The computer program has been developed to select the optimum propeller by considering the boundary condition of the system, hull-propeller interactions, and engine-propeller matching (EPM). This research also carried out open water and self-propulsion simulations using computational fluid dynamics (CFD). Then it can be concluded that the development of an algorithm to optimize the selection of propellers on KMP Dharma Rucitra 3 obtained propellers with B4-49.6 type with a diameter of 1,995 m so that it can reach a speed of 14,2 knots at 85% maximum continuous rating of engine power.

Copyright © 2023 KAPAL : Jurnal Ilmu Pengetahuan dan Teknologi Kelautan. This is an open-access article under the CC BY-SA license (<https://creativecommons.org/licenses/by-sa/4.0/>).

1. Introduction

The ship has the ability to reach a wider area, including remote areas. In addition, the costs incurred when using sea transportation services are more efficient because they can transport goods or people in large quantities at lower prices. Ships are categorized into several types, one of which is a ro-ro passenger ship. One of the ro-ro passenger ships serving the Bali - Lombok ferry route and vice versa is the KMP Dharma Rucitra 3. Ro-ro passenger ship owned by PT. Dharma Lautan Utama is equipped with a twin-screw propulsion system. This ship is powered by a diesel engine manufactured by Makita GNLH 630M with a power of 1300 HP at 375 RPM. On June 12, 2020, at Padangbai Port, Karangasem, Bali, this ship had an accident and almost sank. This causes diesel engines to be submerged in seawater for a long time due to many administrative processes. Thus, causing corrosion on the main engine. Therefore, the Makita GNLH 630M engine will be replaced with an engine that is already in the company's warehouse with the Yanmar 6N21A SV manufacturer, which has a power of 1200 HP at 850 RPM. The reason for using a Yanmar 6N21A SV because the engine is already in the company's warehouse, so the company does not need to buy a new engine.

To achieve the desired speed, it is necessary to have an optimal propeller to improve engine performance. Critical design analysis in a ship propulsion system is the optimal matching of the propeller to the hull interaction. Choosing the right propulsion system to match the hull and engine is a very important decision. The engine propeller matching process considered the interaction between the hull of the ship and the diesel engine. The engine and gear ratio matches when the engine torque and propeller torque are balanced, which means the engine will not overload [1]. To realize the desired speed service, designing the optimal propeller to improve the high engine performance and reduce costs from fuel oil consumption and vibration-induced stresses on the ship [2].

There are three parameters that limit the propeller design, such as propeller diameter, highest propeller efficiency and cavitation phenomenon, cavitation has to be considered and controlled in the design process by the propeller designer, and it has certainly changed how the propeller design is involved. The prime mover is one of the major steps in shipbuilding projects because of is usually operated until the lifetime of the ship [3]. To optimize the prime mover system, the following parameters, type of propulsion, fuel oil consumption, payload, maneuverability, principal main dimension, environment,

etc., must be considered [4]. Reducing fuel consumption, low emission control, noise and vibration due to propeller matching is required [5].

The optimum propeller design problem can be handled using the propeller series diagrams or regression polynomials [6]. This paper addresses improving and evaluating the performance based on the algorithm. The algorithm is applied to find optimal solutions by defining the overall parameters of a propeller-like diameter, pitch-ratio, blade area ratio and the number of blades [7]. This research has input design parameters such as speed service, wake fraction, thrust deduction fraction, total resistance, number of blades, maximum diameter, engine power, service margin, engine margin, and shafting efficiency. Input design parameters for considering hull-propeller interaction and engine-propeller matching, and iterate the variables in the range to get optimum propeller efficiency.

Based on the background that has been mentioned, the authors will analyze the impact of replacing the Makita GNLH 630M engine with the Yanmar 6N21A. This research it is aimed to get the optimum propeller using an algorithm with Microsoft Excel so that the ship can achieve the highest performance.

2. Methods

2.1 Research Method

The methods are the main difficulty in most optimization problems. It defines in formulating the objective all the constraints. Any constrained optimization problem could be handled by the optimization design propeller process shown in Figure 2. Optimum design propeller process impression by hull interaction and engine propeller matching. The correlation between the engine and propeller is shown in the service condition shown in Figure 1. The services condition refers to the mean service conditions that the ship will encounter in its operational life. Good practice involves some hull fouling (e.g., two years), sea state 2 or 3, deep water and design displacement. The operating envelope is used to plot the propeller load at design condition and trial condition with the Engine Margin (EM) and service margin (SM) boundary.

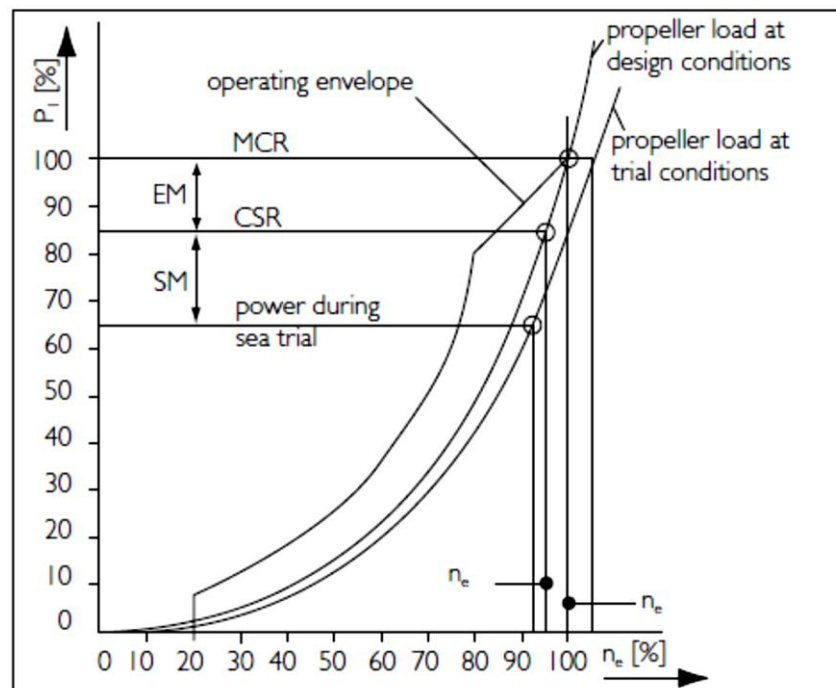


Figure 1. Correlation between Engine and Propeller at Service Condition [8]

The fuel coefficient identifies the fuel flow and log speed. This gives the overall ship performance, including the engine, propeller and hull. The power coefficient identifies the shaft power and logs speed, and this gives the overall efficiency of the propeller and hull, excluding the engine. The specific fuel consumption (SFC), propeller, and hull coefficients isolated the individual components giving the efficiency of each independently.

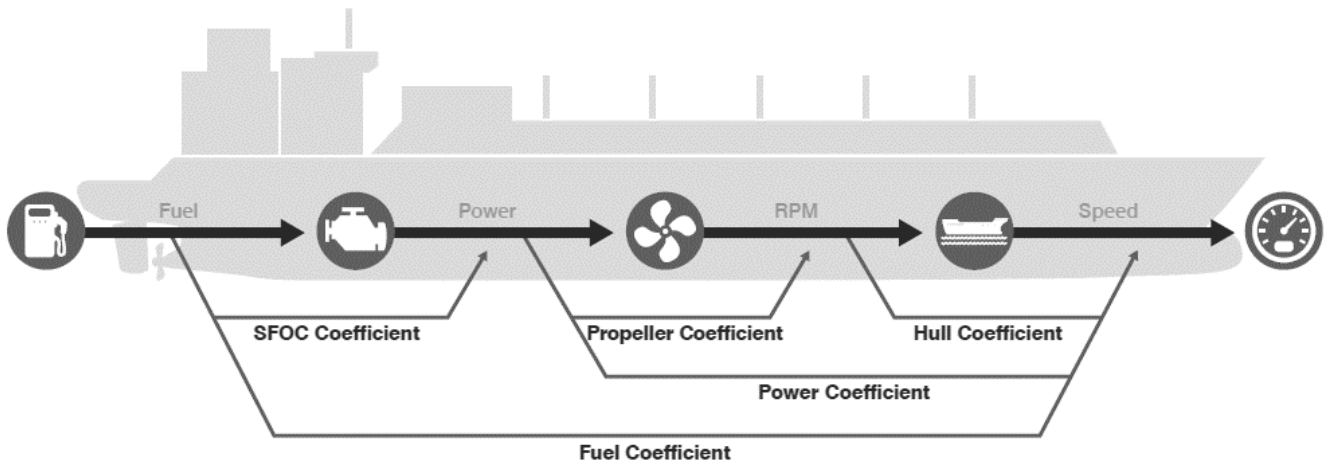


Figure 2. Coefficient parameters for the ship's performance (Fathom world)

Figure 3 below shows the steps of carrying out this research from start to finish in determining the optimum propeller with a new engine, but the speed of the ship can be achieved. The initial stage is to collect data from the old engine with the new engine, as well as data from the KMP Dharma Rucitra 3 ship. The shape and characteristics of the ship have not changed, but with the presence of a new engine that has different characteristics from the old engine, it is necessary to make adjustments to the ship's propulsion system, with the hope that the speed of the ship can be achieved. In this research, the focus is on the propeller selection process (including the efficiency, diameter and cavitation of the propeller) and also the calculation of engine propeller matching, which can be optimized.

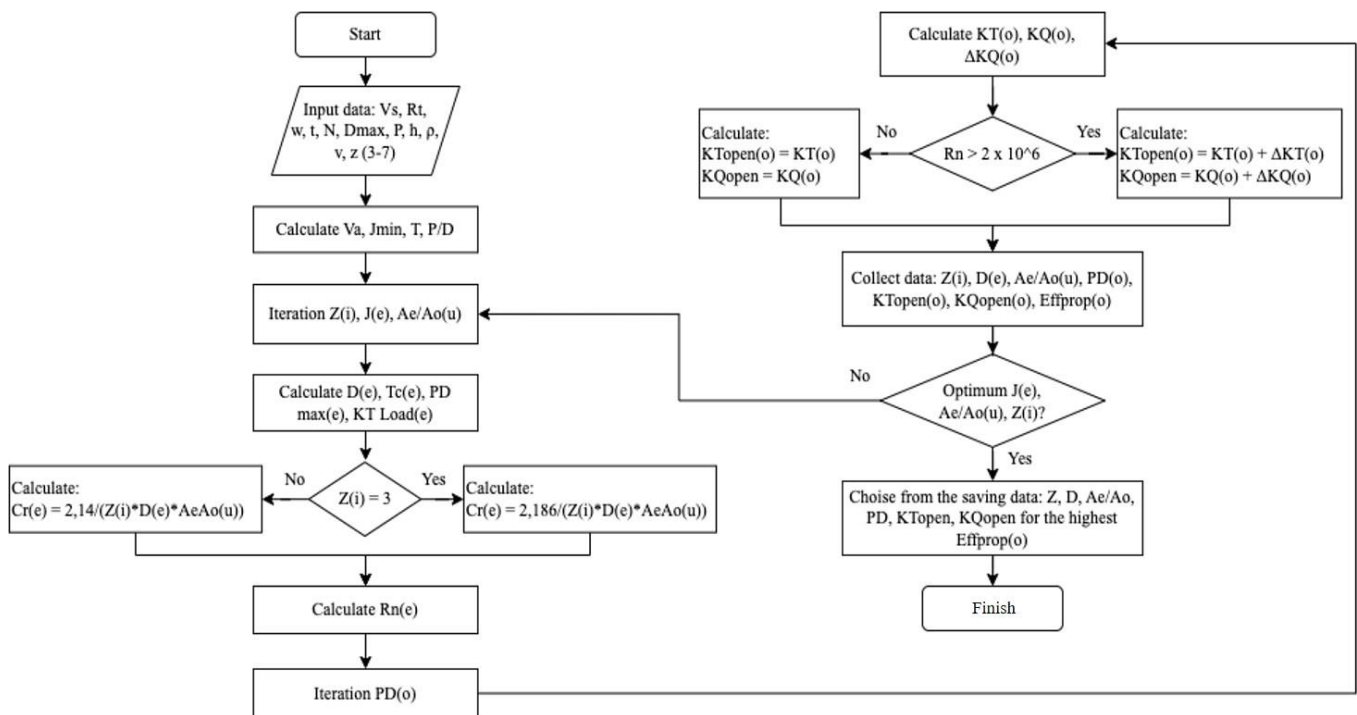


Figure 3. Methodology

Integrating a propeller, ship hull and the engine is called engine propeller matching. The total resistance of the ship with a certain speed must be known. It means the torque and thrust of the propeller selection overcome the resistance and engine that match the propeller. The basic data of propeller design in order to introduce the relationship between the propeller diameter (D), velocity (Vs), advance velocity (Va), wake friction parameters (w), the rate of revolution (n), the density of the water (ρ), of which important coefficients are discussed below [9,10].

The advance velocity.

$$V_a = V_s(1 - w) \tag{1}$$

Where;

V_a : advance velocity, m/s

V_s : service velocity, m/s

w : wake friction

The thrust calculation.

$$T = K_T \cdot \rho \cdot n^2 \cdot D^4 \quad (2)$$

$$T = \frac{R_t}{(1-t)} \quad (3)$$

Where;

T : thrust, kN

K_T : thrust coefficient

ρ : water density, kg/m³

n : rotation of propeller, rotation per second

D : diameter of propeller, m

R_t : resistance, kN

t : thrust deduction

The thrust coefficient.

$$K_T = \frac{R_t}{(\rho \cdot n^2 \cdot D^4 \cdot (1-t))} \quad (4)$$

Where;

K_T : thrust coefficient

ρ : water density, kg/m³

n : rotation of propeller, rotation per second

D : diameter of propeller, m

R_t : resistance, kN

t : thrust deduction

The propeller load characteristic.

$$K_T = \left[\frac{R_t}{(V_a^2 \cdot \rho \cdot D^2 (1-t))} \right] \cdot J^2 \quad (5)$$

$$K_T = \left[\frac{R_t \cdot n^2}{(V_a^4 \cdot \rho \cdot (1-t))} \right] \cdot J^4 \quad (6)$$

Where;

K_T : thrust coefficient

ρ : water density, kg/m³

n : rotation of propeller, rotation per second

D : diameter of propeller, m

R_t : resistance, kN

t : thrust deduction

V_a : advance velocity, m/s

J : Advanced coefficient

Advance coefficient.

$$J = \frac{V_a}{(n \cdot D)} \quad (7)$$

Where;

n : rotation of propeller, rotation per second

D : diameter of propeller, m

V_a : advance velocity. m/s

The propeller torque.

$$K_Q = \frac{Q}{\rho \cdot n^2 \cdot D^5} \quad (8)$$

Where;

K_Q : torque coefficient

ρ : water density, kg/m³

n : rotation of propeller, rotation per second

D : diameter of propeller, m

Q : torque, Nm

Based on the propeller diagrams is possible to calculate the propeller size, the shaft power and the efficiency, which are amongst J, K_T , and K_Q curves, off design conditions which the operating aspect of the propeller can be analyzed from open water diagrams [11, 12]. This step is used to progress further in solving some off-design propeller that affects the operational envelope [13]. Propeller characteristic parameters K_T , K_Q , η values depend on the number of blades (Z) from 2 to 7, area ratio (A_e/A_o) from 0,2 to 1,05, pitch diameter ratio (P/D) from 0,47 to 1,5 and advance coefficient (J).

The polynomial equations for the B-Series propeller will be used to plot the open water characteristics, number of blade ranges, blade area ratio and the ratio of pitch diameter [14]. The polynomial equation explains the correlation between thrust and torque coefficient in terms of the number of blades, blade area ratio, advance coefficient and the ratio of pitch diameter. The polynomial equation with multiple regression is:

$$K_T = \sum_{s,t,u,v} c_{s,t,u,v}^T (J)^s (P/D)^t (A_E/A_0)^u (Z)^v \quad (9)$$

$$K_Q = \sum_{s,t,u,v} c_{s,t,u,v}^Q (J)^s (P/D)^t (A_E/A_0)^u (Z)^v \quad (10)$$

$$\eta = \frac{K_t}{K_q} \frac{J}{2\pi} \quad (11)$$

Where;

K_T : thrust coefficient

K_Q : torque coefficient

J : Advanced coefficient

η : efficiency, %

Z : number of blades

P/D : pitch diameter ratio

A_e/A_o : area ratio

The parameter of characteristics of open water tests such as K_T , K_Q , η_o , J , and P/D can be seen in equations (1) and (12). The advance ratio (J), wake friction (w) and rotation of the propeller are determined as a ship speed function. The boundary condition of the stern ship space is the maximum diameter affected by the advance ratio J .

$$J_{min} = V_a / (n D_{max}) \quad (12)$$

Where;

J : minimal advance coefficient

n : rotation of propeller, rotation per second

V_a : advance velocity, m/s

D_{max} : maximal diameter of propeller, m

Cavitation on the back of propeller blades was constrained according to the Burril diagram [15]. Cavitation is defined as the process of the vapor phase of a liquid when it is subjected to reduced pressure at constant ambient temperature. It occurs when large suction pressures build up near the leading edge of the blade resulting in the back of the blade being covered with a sheet of bubbles [16]. The thrust loading coefficient must be less than the maximum thrust loading coefficient and maximum cavitation level adopted by Table 1. The boundary condition of cavitation can be calculated by using the formula (13).

Table 1. Manufacturing Accuracy of Propellers [13]

Class	Manufacturing Accuracy	Mean Pitch for Propeller
S	Very high accuracy	± 0.50 %
1	High accuracy	± 0.75 %
11	Medium accuracy	± 1.00 %
111	Wide tolerance	± 3.00 %

$$\sigma_{0.7R} = \frac{188.2 + 19.62 h}{V_A^2 + 4.83 n^2 D^2} \quad (13)$$

$$n^2 D^2 = \frac{V_a^2}{J^2} \quad (14)$$

The critical thrust coefficient can be calculated by using the formula (16).

$$\tau_{c-limit} = f(\sigma_{0.7R}) = f(J) \quad (15)$$

$$\tau_c = \frac{T}{\frac{1}{2} \rho V_R^2 A_p} \quad (16)$$

Where;

A_p : the projected area, m

A_d : the developed area, m

V_a : advance velocity, m/s

n : rotation of propeller, rps

D : propeller diameter. m

$$A_p = \frac{(1.067 - 0.229 \frac{P}{D})}{A_d} \quad (17)$$

4. There are two boundary conditions of this calculation, minimum advance number and ratio of P/D_{max} , shown in Figure

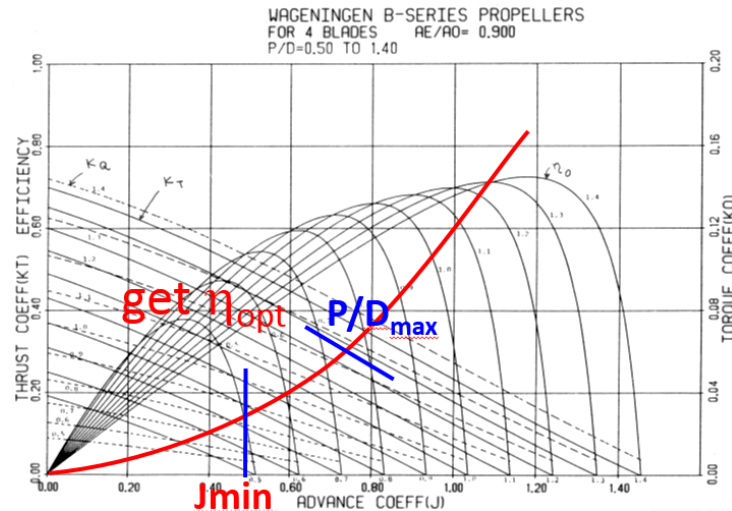


Figure 4. Boundary condition to choose datapoints

$$J_{min} = Va(n D_{max}) \quad (18)$$

$$\frac{P}{D_{max}} = f(J) \quad (19)$$

$$Propeller\ Speed = Max.Speed \times (1 - EM)^{\frac{1}{m}} \quad (20)$$

$m \approx 3$

In this research, the development of the algorithm starts with selecting engines and gearboxes that are applicable to the propulsion system. Estimated power can be calculated by:

$$Power = (R_r \cdot V_s) / (\eta_H \eta_O \eta_R \eta_S \eta_{gb}) \quad (21)$$

The formula added by SM & EM where η_o depends on the type of ship. After selecting the engine, input design parameters such as V_s , w , t , R_r , number of blades, diameter maximum, engine power & speed, SM, EM, and shafting efficiency. Change all equations as a function of design parameters and variables Z , A_e/A_o , P/D , J . For considering hull-propeller interaction and engine-propeller matching, iterate the variables in the range to get optimum propeller efficiency.

2.2 Tools used in research

The tools used during the propeller optimization are a solver using Microsoft Excel software and computational fluid dynamics (CFD) using Numeca software.

1. Solver

The algorithm that has been developed to select the optimal propeller uses the solver in adds-in on Microsoft Excel. This is because it simplifies the calculation process in accordance with the methodology. Solver makes the system consider the desired result without ignoring the variables within predetermined limits.

2. Computational Fluid Dynamics (CFD)

Because the input data for the solver uses assumed values for the wake and thrust deduction, it is necessary to carry out a simulation in the form of a self-propulsion test with CFD. The simulation uses a disk actuator so that input is needed in the form of K_T , K_Q , and J values from the open water simulation.

3 Results and Discussion

3.1 Ship Resistance

Initially, the ship's resistance at each speed was calculated using the Holtrop method, maxsurf Holtrop, and CFD simulation methods. However, the data taken for further processing is the maxsurf Holtrop resistance, whose value has been matched whether it is close to the Holtrop method. Furthermore, the resistance value from CFD simulation is validated by Holtrop maxsurf. So, it is ensured that for each resistance, it must be close, with a difference of $\pm 5\%$. The simulated speed using CFD is from 11 to 15 knots. Figure 5 is a comparison of the resistance value of maxsurf simulation (Holtrop method) and CFD simulation.

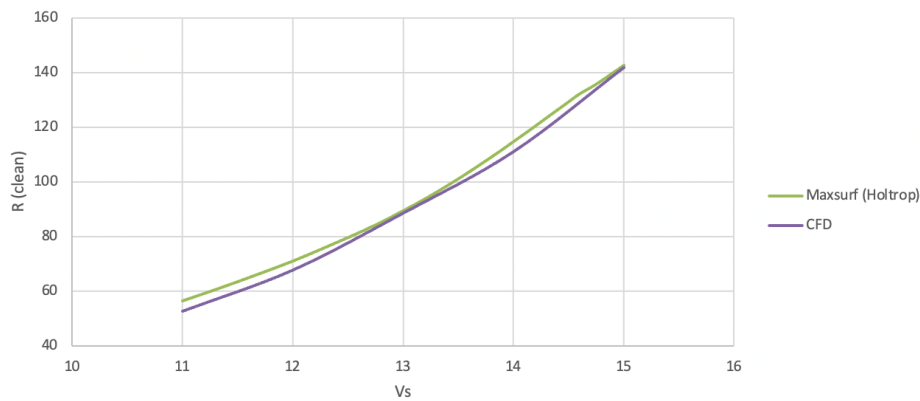


Figure 5. Ship resistance value from Holtrop method, maxsurf software, and CFD simulation at various speed

3.2 Propeller Optimization

Because KMP Dharma Rucitra 3 is being repowered with the new engine, Yanmar 6N21A SV, with a power of 1200 HP at 850 RPM, it is necessary to change the propeller as well to achieve the highest performance. The selection of a new propeller is made by optimizing using an algorithm. Firstly, an optimization algorithm that is capable of developing the engine propeller matching process considering hull-propeller interaction and engine-propeller matching. An algorithm step is based on algorithmic development. There are many ways to fill in these steps, depending on the problem in the case. The algorithm contains the basic part that was given in methodology Figure 3. This characteristic can be found in the selection and replacement part of the algorithm. The main steps, as shown in Figure 3, are now explained in more detail.

Table 2. Input Data

Input Data	Value	Unit
Ship resistance, R_t	53,85295	kN
Ship speed, V_s	13,75	knot
Block coefficient, C_b	0,628	
Engine power, P	882,5985	kW
Wake deduction factor, W	0,02828	
Thrust deduction factor, T	0,14707	
Max. propeller diameter, D_{max}	2,65	m
Height, H	1,809	m
Rotation, N	5,6413591	rps
Sea water density, ρ	1025	kg/m ³
Kinematic viscosity at 27C	0,00000087	m/s ²
Allowable Stress Material (Manganese Bronze)	39	Mn/m ²
Number of blades, Z	4-7	

The optimization process is the objective function of selecting the propeller that has the most optimal performance and design variables as propulsion parameters. Component design characteristics refer to the propeller and engine data specification that will be input in the first step of the process. All of the computations were executed by the solver on Microsoft Excel. The aim approach shows an overview of each calculating model. The first step of algorithmic development is to input the hull information, ship, engine, and propeller data such as speed V_s , resistance R_t , wake friction w , maximum propeller diameter D_{max} , ratio gearbox R_{gb} , etc. Table 2 shows the input data of the algorithm process. With the above-given data, a matching pitch is achieved, with another case representing a range of pitch ratios. The information defined in the open water diagram is achieved, which is used to construe the open water efficiency curve, torque coefficient, thrust coefficient, total resistance, and advance ratio.

The variation in coefficient is a sign that various case of the ship affects the performance of the hull-propeller interaction and engine-propeller matching. Constraint the iteration $Z(i)$ from 3 to 7 with interval 1, iteration $Ae/Ao(u)$: from J_{min} to 1,05 with interval 0,01 and iteration $J(e)$: from J_{min} to 1,5 with interval 0,01. Thrust and torque coefficient of the Wageningen B-series are delivered as polynomials in the advance ratio J , the pitch ratio P/D , the blade area ratio Ae/Ao , and the number of blades Z . Then, calculate the propeller performance such as $D(e)$, $Tc(e)$, $P/D_{max}(e)$ and $K_{T load}(e)$. Reynolds number R_n is calculated in the polynomials, the correlation shown in equation (9) and equation (10).

One of the excesses of the applied optimization algorithm is obtaining various design data, even of only one. This is necessary for making the final decision. For example, the pitch of the propeller change based on the value of J , K_T , K_Q , and η_0 .

which sign the effect of pitch ratio on the hydrodynamic curve of the propeller design. Table 3 shows the result of the optimization algorithm for each propeller blade.

	Z=4	Z=5	Z=6	Z=7
Maximal diameter, Dmax	2,65	2,65	2,65	2,65
Diamater Propeller, D	1,9831622	1,88757248	1,8726362	1,8112626
Face Pitch Ratio, P/D	0,8198936	0,8998101	0,9094749	0,9819309
Advance Coefficient, J	0,6138538	0,64494039	0,6500845	0,6721122
Blade Ratio, Ae/Ao	0,4937391	0,58663852	0,6296112	0,6527621
Propeller Efficiency	62,307%	59,751%	57,346%	55,420%
J _{min}	0,459386	0,459386	0,459386	0,459386
(t _{min} /D)0.7R	0,007556	0,007853	0,007906	0,008085
Tmax	0,0156	0,0141	0,0126	0,0111
KT load	0,125133	0,152472	0,157395	0,179837
KT	0,125125	0,152155	0,157077	0,186909
KQ	0,01963	0,026152	0,028354	0,036095
Rotation n output	5,641359	5,641359	5,641359	5,641359
Rotation n input	5,641359	5,641359	5,641359	5,641359
Rotation n deviation	0	0	0	0
Thrust, T	63,13483	63,00741	63,01117	65,62176
Torsion, Q	19,64258	20,44142	21,29989	22,95346
Torsion, Qb	19,70169	20,50293	21,36398	23,02252
Delivery Horse Power, DHP	697,9862	726,3724	756,8774	815,6359
Brake Horse Power, BHP _{scr}	734,2585	764,1199	796,2102	858,0222

From the four propellers in Table 3, the propeller that has an 85% maximum continuous rating of engine power for the Yanmar 6N21A SV engine is selected, namely the B4 propeller with Ae/Ao 0,493. From the type of propeller obtained, then draw the new open-water propeller diagram. This open water diagram is used to find power and rotation for each speed using B4-49.3 propellers with new engines. The following Figure 6 is an open water propeller diagram for the new B4-49.3.

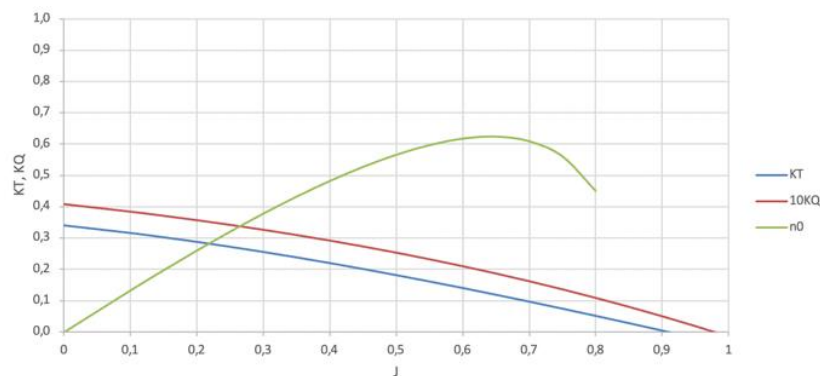


Figure 6. B4-49.3 propeller open water diagram

For each speed, power and rotation are calculated based on the old B4-49.3 open water propeller diagram. By finding the intersection of the rough hull values for each speed, the KT Open, KT Load, and KQ values can be calculated where the value of KT Open and KT Load must be zero. This value can be searched using the Microsoft Excel feature using goal seek in what-if analysis. After that, the value of rotation and power can be calculated. The rotations and power are tabulated, making it easier to plot on the engine envelope graph. In Figure 7, it can be seen in the curve named B4-49.3 that at 85% brake horsepower (BHP), it can reach a speed of 13,75 knots with a rotation of 797,6 rpm. So that it can be said that the engine propeller matching means that the operating point of the ship's engine rotation is such that it matches the propeller loads B4-49.3.

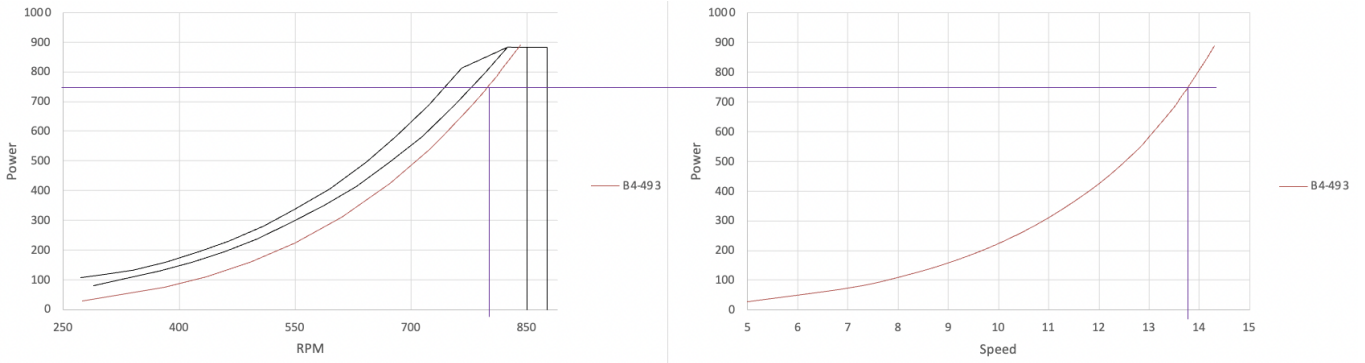


Figure 7. B4-49.3 Propeller curve and speed-power curve

3.3 Self-propulsion Test

The value of the wake and thrust deduction factor as input data for the optimization algorithm is assumed, so it is necessary to look for values derived from the self-propulsion test. By testing the hull and propeller simultaneously in the same domain, the fluid interaction between the hull and propeller will be known. In this simulation, the input used is the ship's speed and K_T , K_Q , and J from output values in the open water test. So firstly, simulating open water test as the input of self-propulsion test. An open water test simulates a propeller selected with fixed propeller rotation on 5,6414 rps, various advance speeds (V_a), and various advance coefficients (J) using the CFD method. Inputted values of V_a are 4,4751 m/s, 5,5939 m/s, 6,7127 m/s, 7,8315 m/s, and 8,9503 m/s, while the inputted value of J from 0,4 to 0,8 with 0,1 interval. Before running this simulation, it is necessary to do meshing first to define the propeller so that it is divided into several nodes and elements. Meshing in this simulation has a total of 627,388 cells. The meshing and test results are shown in Figure 8 as follows.

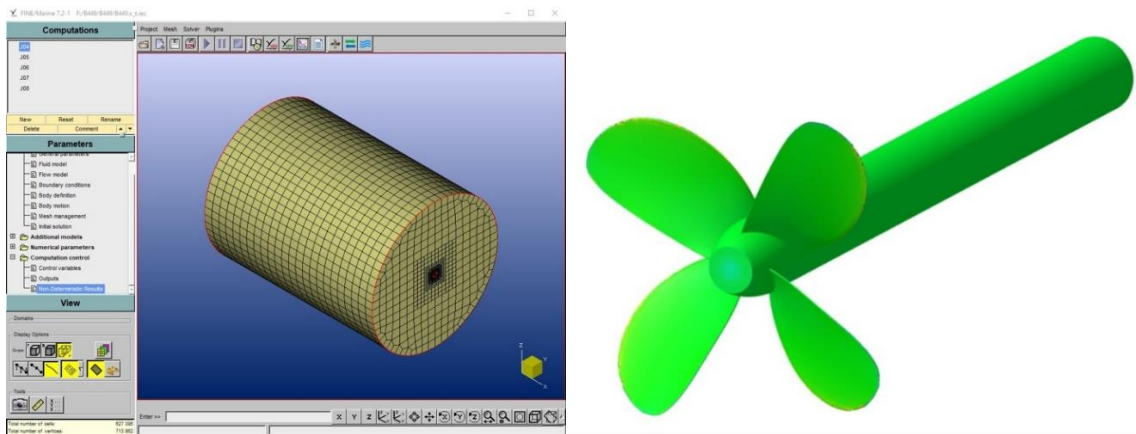


Figure 8. Open water test meshing and propeller geometry

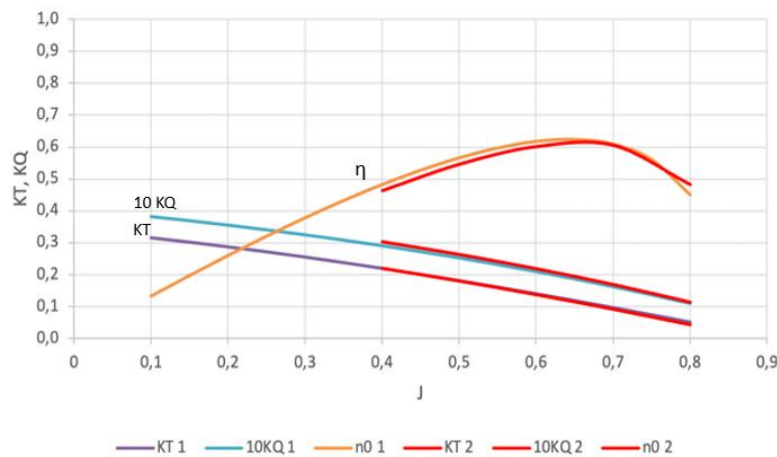


Figure 9. Open water diagram validation

With this simulation, output data such as thrust (T) and torque (Q). This value can be seen on the monitor start menu in the Fine Marine software. The thrust value is in the forces section, while the torque value is in the moment section. Validation will be accepted if the difference of each coefficient is $\pm 5\%$. From the calculation, the validation of the data can be accepted. Figure 9 is the polynomial and simulation open water diagram. Figure 9 shows a comparison of the values of K_T , K_Q and efficiency between polynomial calculations and simulations in open water conditions. From the figure, it can be seen that if the value of J is between 0.4 to 0.65, then the value of the simulation efficiency is greater than the calculation. While

for 10KQ & KT, the simulation value is smaller than the calculation. For values between 0.65 and 0.8, both scenarios produce almost the same results.

After K_T , K_Q , and J is obtained, then calculating the ship's speed is an input of the self-propulsion test. The ship's speed is obtained by calculating the engine propeller matching between the new engine and propeller B4-49.3 using clean hull resistance. In this simulation, the propeller used is in the form of a disk actuator so that in modeling, the data will be input from the open water test. As with the open water simulation, before running the self-propulsion simulation, it is necessary to do meshing first to define the propeller so that it is divided into several nodes and elements. Meshing in this simulation has a total of 2,264,592 cells. The test results are shown in Figure 10 as follows.

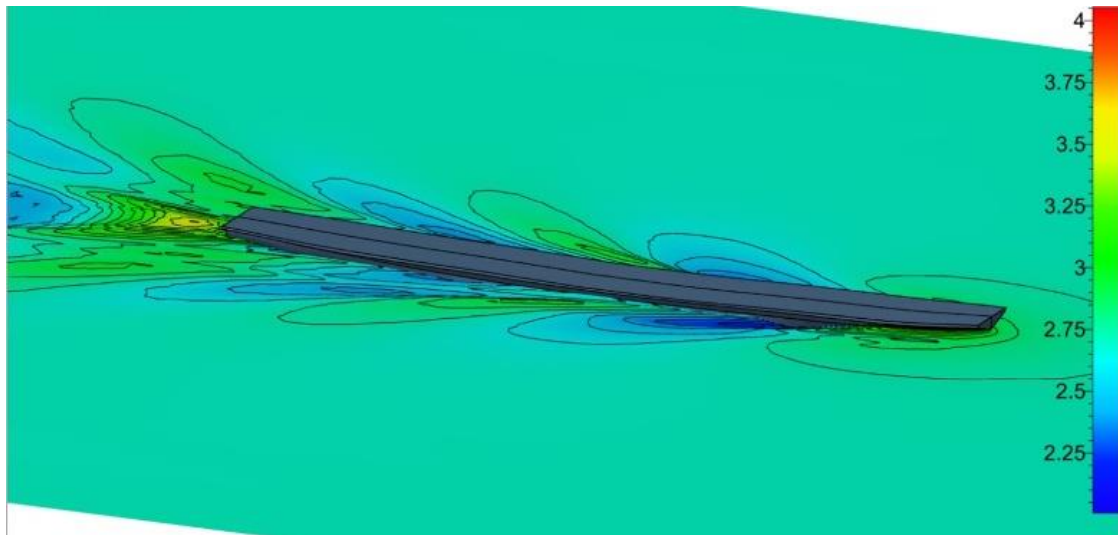


Figure 10. Self-propulsion test simulation

From this simulation, the values of n , K_T , K_Q , and J are obtained as the output. This value can be seen on the monitor start menu in the Fine Marine software. The output value shown in Figure 11 is that n is 5,59 rps, K_T is 0,112819, K_Q is 0,019205, and J is 0,654638.

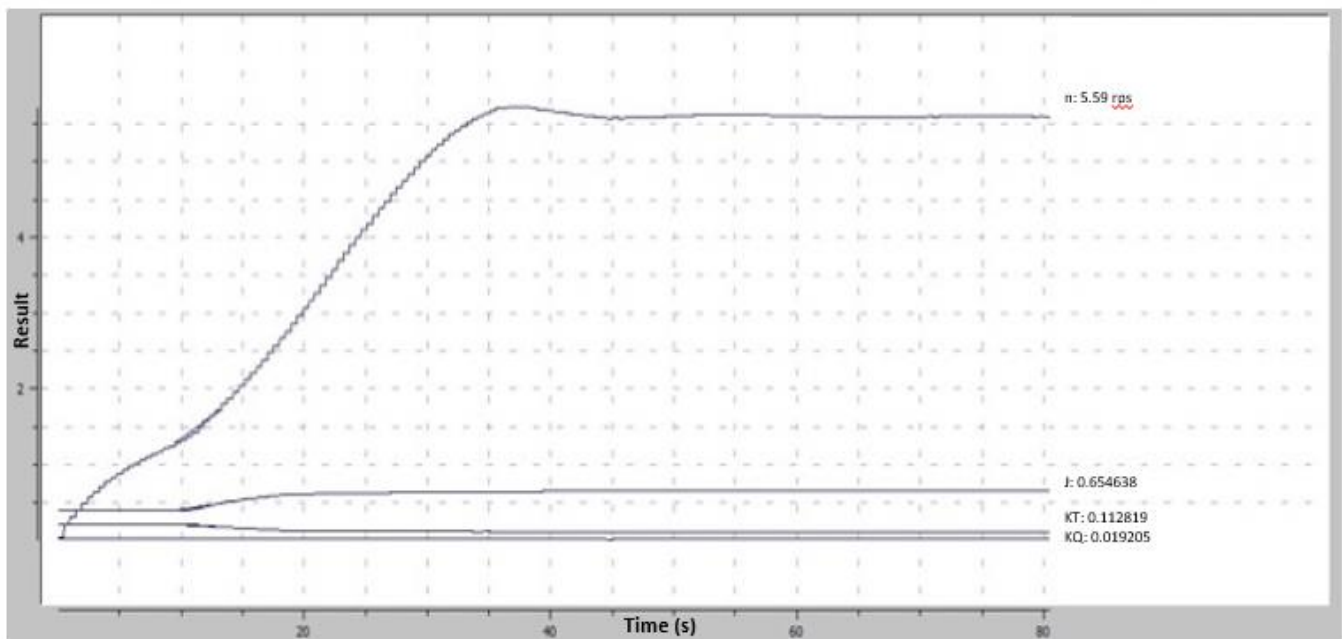


Figure 11. The output value of the self-propulsion test

From the output value, advance velocity would be obtained and then would be used to calculate wake with the following formula: [17-19]

$$\begin{aligned}
 V_a &= n \times J \times D & (23) \\
 V_a &= 5,59 \times 0,654 \times 1,983 \\
 V_a &= 7,2573 \\
 w &= 1 - \frac{V_a}{V_s} \\
 w &= 1 - \frac{7,2573}{7,588}
 \end{aligned}$$

$$w = 0,04357$$

(24)

Thrust from the self-propulsion test would be used to calculate thrust deduction factor (t) using the following formula: [17-19]

$$t = \frac{T - R_t}{T} \tag{25}$$

$$t = \frac{54080,58 - 52314,7}{54080,58}$$

$$t = 0,032653$$

Initially, the wake and thrust deduction values were only assumptions, with values of 0,02828 and 0,1471, respectively. This value is different from the simulation results. Therefore, optimization of the selection of new propellers is carried out using the new wake and thrust deduction factor values as inputs. Then the propeller results are obtained with type B4-49.6 because, in the beginning, it used the assumption on the value of wake and thrust. The following is Table 4, which contains data from propellers with simulated w and t values, namely B4-49.6, meanwhile propeller data with assumed w and t values, namely B4-49.3.

Table 4. Propeller data of B4-49.3 and B4-49.6

Data	Propeller B4-49.3	Propeller B4-49.6
Diameter (m)	1,98316	1,995
P/D	0,81989	0,8272
Ae/Ao	0,49372	0,4968

From the type of propeller obtained, then draw the new propeller open water diagram. Figure 12 is the open water diagram.

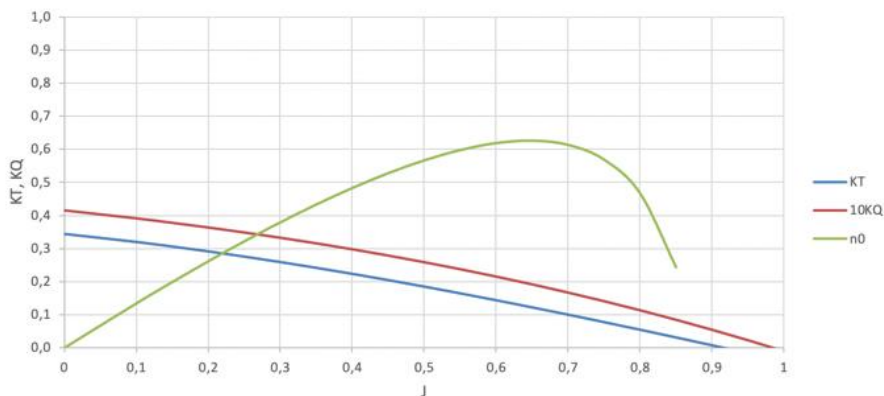


Figure 12. B4-49.6 propeller open water diagram

Then, from the diagram, we can look for the rotation and power that can be achieved by a ship's speed in the same way as on the previous propeller. The rotations and power are tabulated, making it easy to plot on an engine envelope graph. Figure 13 shows a graph of the propeller curve and speed-power curve.

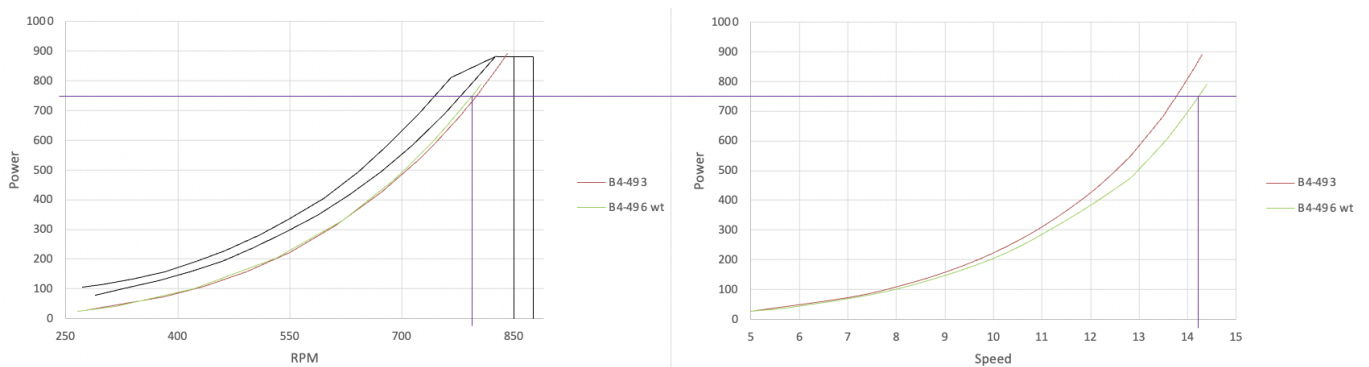


Figure 13. Propeller curve and speed-power curve of B4-49.6

Figure 13 shows the curve named B4-49.6 at 85% BHP can reach a speed of 14,2 knots. So that it can be said that the B4-49.6 propeller matches the Yanmar engine, meaning that the operating point of the ship's engine rotation is such that it matches the propeller load. Then the curve shows that the power value is lower than the power value on the curve named B4-49.3 because it has a different thrust deduction (t) value. The t value used on the propeller B4-49.6 is the result of a

simulation is 0,032, while the propeller B4-49.3 uses the assumed t value of 0,147. The t value has decreased, so the power value has also decreased. The thrust deduction value decreases because the position of the propeller and the hull is far away, which causes the eddy resistance to decrease. Eddy resistance is caused by the changing pressure around the ship due to changes in velocity induced by the eddies of the stream separating from the hull surface.

Then from the new B4-49.6 propeller, a self-propulsion simulation was carried out to find the wake and thrust deduction values for the propeller. The wake and thrust deduction values are 0,035 and 0,071, respectively. This value has differences from the value in the first simulation with the B4-49.3 propeller because of the difference in input for the type of propeller and the speed that the ship can achieve due to the new propeller, for the self-propulsion simulation results of B4-49.6 propeller can be seen in Figure 14.

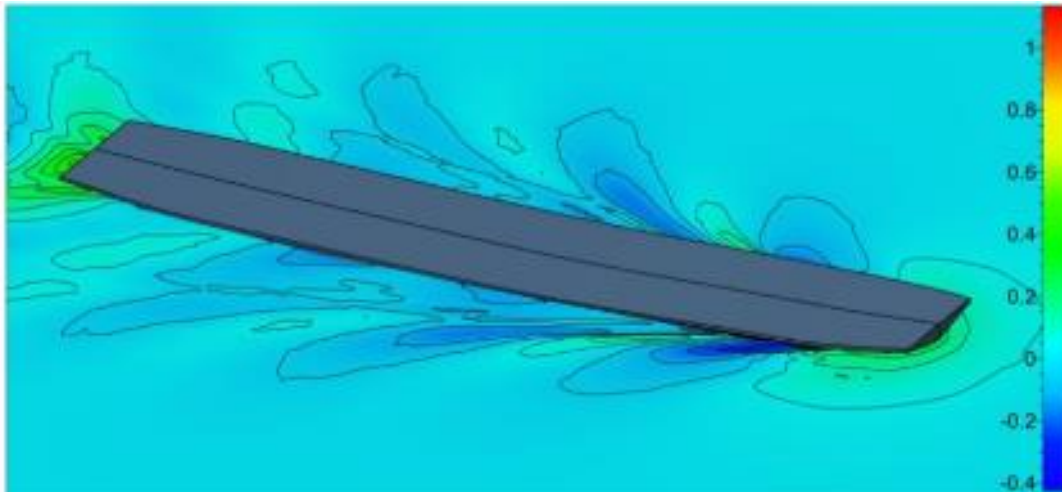


Figure 14. Self-propulsion test simulation

4 Conclusion

Based on the analysis of calculations and simulations in this research, it can be concluded that the development of an algorithm to optimize the selection of propellers on KMP Dharma Rucitra 3 obtained propellers with B4 type with A_e/A_o ratio is 0,496, propeller diameter 1,995 m and P/D ratio is 0,8272. Optimization of the propeller selection was carried out using the simulated wake deduction value is 0,0435 and thrust deduction value is 0,0326. The propeller can reach a ship's speed of up to 14,2 knots at 85% of the engine's brake horsepower.

Acknowledgments

The author would like to thank the staff of the Marine Power and Propulsion Laboratory and PT Dharma Lautan Utama for their support so that the author can complete the research.

References

- [1] O. B. Ogar, S. Nitonye and I. J. Hope, "Design Analysis and Optimal Matching of a Controllable Pitch Propeller to the Hull and Diesel Engine of a CODOG System," *Journal of Power and Energy Engineering*, vol. 6, pp. 53-74, 2018.
- [2] N. Samson, "Numerical Analysis for the Design of the Fuel System of a Sea Going Tug Boat in the Niger Delta," *World Journal of Engineering Research and Technology*, vol. 3, pp. 161-177, 2017.
- [3] C. Marques, C. Belchior and J. Caprace, "Optimising the Engine-Propeller Matching for a Liquefied Natural Gas Carrier under Rough Weather," *Journal of Applied Energy*, vol. 232, pp. 187-196, 2018.
- [4] G. Grunditz, "Optimizing Propeller and Propulsion, the Quest for Reduced Fuel Consumption, Emission and Noise Level," *Journal of Marine Technology*, pp. 49-55, 2015.
- [5] P. Cudina, Analysis of the Energy Efficiency Design Index (EEDI) with a Proposal for Improvement, 2015.
- [6] M. M. Gaafary, H. El-Kilani and M. Moustafa, "Optimum Design of B-Series Marine Propellers," *International Journal of Alexandria Engineering*, vol. 50, pp. 13-18, 2011.
- [7] C. Pouw, "Development of a Multiobjective Design Optimization Procedure for Marine Propellers," Delft University of Technology, Delft, 2007.
- [8] D. Stapersma and H. K. Woud, "Matching Propulsion Engine with Propulsor," *Journal of Marine Engineering & Technology*, vol. 4, pp. 25-32, 2014.
- [9] C. Kusuma and I. M. Ariana, "Desain Propeller Kapal Selam 29 meter dengan Menggunakan Propeller B-Series," *Wave: Jurnal Ilmiah Teknologi Maritim*, vol. 11, pp. 1-6, 2017.
- [10] C. Kusuma and I. M. Ariana, "Studi Numerik Optimasi Propeller Kapal Selam 29 meter dengan Menggunakan High Skew," *Rekayasa Energi Manufaktur Jurnal*, vol. 2, pp. 1-5, 2017.
- [11] A. Oloan, I. M. Ariana and A. Baidowi, "Self Propulsion Performance Analysis of Japanese Bulk Carrier with PBCF based CFD Method," *IOP Conference Series Earth and Environmental Science*, vol. 1081, pp. 1-10, 2022.

- [12] I. M. Ariana, R. Prihandanu, D. W. Handani and A. A. B. Dinariyana, "Investigation of the Effect of the Pre-Duct in a Ship on Propeller-Hull Interactions using the CFD Method," *CFD Letters*, vol. 15, pp. 17-30, 2023. <https://doi.org/10.37934/cfdl.15.4.1730>
- [13] K. Kuiken, "Ship Propulsion and Propellers. In: Diesel Engines II for Ship Propulsion and Power Plants," *Journal of Energy*, pp. 378-395, 2008.
- [14] M. W. C. Oosterveld, "Further Computer-Analyzed Data of the Wageningen B-Screw Series," *Journal International Ship Building Progress*, vol. 22, pp. 251-261.
- [15] J. Carlton, *Marine Propeller and Propulsion*, Oxford, UK: Elsevier BV, 2012.
- [16] P. Eisenberg, "Cavitation," *Hydronautics*, pp. 121-128.
- [17] E. V. Lewis, *Principles of Naval Architecture*, New Jersey, US: The Society of Naval Architects and Marine Engineers, 1989.
- [18] A. Firdhaus, I. K. Suastika, K. Kiryanto, and S. Samuel, "Benchmark Study of FINETM/Marine CFD Code for the Calculation of Ship Resistance," *Kapal: Jurnal Ilmu Pengetahuan dan Teknologi Kelautan*, vol. 18, no. 2, pp. 111-118, Jul. 2021. <https://doi.org/10.14710/kapal.v18i2.39727>
- [19] D. Endro W, "High Speed Ship Total Resistance Calculation (An Empirical Study)," *Kapal: Jurnal Ilmu Pengetahuan dan Teknologi Kelautan*, vol. 11, no. 1, pp. 13 - 20, Feb. 2014. <https://doi.org/10.14710/kpl.v11i1.6338>